Microchim Acta (2012) 176:101–107
DOI 10.1007/s00604-011-0695-z

ORIGINAL PAPER

Highly sensitive detection of lead(II) ion using multicolor CdTe quantum dots

Wenying Zhong · Cui Zhang · Qin Gao · Hui Li

Received: 26 April 2011 / Accepted: 9 September 2011 / Published online: 27 September 2011

Abstract Multicolor and water-soluble CdTe quantum dots (QDs) were synthesized with thioglycolic acid (TGA) as stabilizer. These QDs have a good size distribution, display high fluorescence quantum yield, and can be applied to the ultrasensitive detection of Pb (II) ion by virtue of their quenching effect. The size of the QDs exerts a strong effect on sensitivity, and quenching of luminescence is most effective for the smallest particles. The quenching mechanism is discussed. Fairly selective detection was accomplished by utilizing QDs with a diameter of 1.6 nm which resulted in a detection limit of 4.7 nmol L^{-1} concentration of Pb(II). The method was successfully applied to the determination of Pb(II) in spinach and citrus leaves, and the results are in good agreement with those obtained with atomic absorption spectrometry.

Keywords CdTe quantum dots (QDs) · Multicolor · Fluorescence quenching · Lead(II)

Introduction

Contamination by heavy metal ions, particularly Pb^{2+}, poses a serious threat to the environment and human health. If blood lead levels exceed the provided standard (0.48 μmol L^{-1}), mental development could be impaired, indigestion could occur, and renal functions could be compromised [1, 2].

To date, several methods have been developed for the determination of Pb^{2+}, including high-performance liquid chromatography [3], flame atomic absorption spectrometry (AAS) [4], inductively coupled plasma-mass spectrometry [5], turbidimetry [6], and inductively coupled plasma atomic emission spectrometry [7]. However, these methods are generally time-consuming and expensive, and require further improvements. Because these defects limit the practical application of the existing methods, it is necessary to develop a rapid, economical, and sensitive method for the detection of Pb^{2+}.

For nearly three decades, quantum dots (QDs) have been rapidly developing because of their unique advantages. Compared with traditional organic dyes, QDs have excellent optical properties, such as higher fluorescence intensity, photochemical stability, a tunable emission spectrum, and a narrower spectral line-width. QDs have attracted wide interest due to their various potential applications in drug screening, cell imaging, and biomarking [8–12], among others. Recent advances in QDs show great promise in molecular detection, including compounds with Cu^{2+} [13,

Electronic supplementary material The online version of this article (doi:10.1007/s00604-011-0695-z) contains supplementary material, which is available to authorized users.

W. Zhong (✉) · C. Zhang
Department of Analytical Chemistry,
China Pharmaceutical University,
Nanjing 210009, China
e-mail: wyzhong@cpu.edu.cn

Q. Gao
Agricultural Products Inspection Center of Jiangsu Province,
Nanjing 210036, China

H. Li
School of Chemistry and Chemical Engineering,
Nanjing University,
Nanjing 210093, China

14], Au^{3+} [15], Ag^{+} [16], Co^{2+} [17], Hg^{2+} [18], Fe^{2+}, and Fe^{3+} [19]. The use of QDs in food analysis is also an emerging field [20]. Unfortunately, few reports have been published regarding the detection of Pb^{2+} with QDs. For example, Wu et al. [21] detected Pb^{2+} using thiol-capped CdTe QDs with a detection limit of 2.7×10^{-7} mol L^{-1}.

In this paper, water-soluble thioglycolic acid-capped CdTe QDs are used as fluorescent probe to detect Pb^{2+}. The relationship between the QD size and the detection sensitivity of Pb^{2+} is studied in detail, and the mechanism of interaction between the five colors of CdTe QDs and Pb^{2+} is systematically explored. In addition, the influence of six other coexisting ions on the fluorescence signal of Pb^{2+} is also determined. A novel platform for selective detection by utilizing CdTe QDs as fluorescence probes is developed. This platform is based on the quenching fluorescence of CdTe QDs. The smallest particle, CdTe QDs-I, is chosen to detect Pb^{2+} in spinach and citrus leaves. Compared with Ref. [21], the use of our method increases Pb^{2+}sensitivity by almost 180-fold.

Experimental

Apparatus and chemicals

Fluorescence measurements were performed using an RF-5301 spectrofluorometer (Shimadzu, Japan). UV absorption spectra were recorded with a 3100 UV-Vis spectrophotometer (Shimadzu, Japan). Transmission electron micrography (TEM) was performed on a JEM-2100 system operating at an acceleration voltage of 200 kV (Japan). X-ray powder diffraction (XRD) spectra were taken on a XRD-6000 system (Shimadzu, Japan). Graphite furnace atomic absorption spectra were obtained with a Wa Li-An AA220 instrument (China).

Doubly deionized water was used throughout the experiment. Thioglycolic acid was purchased from Shanghai Lingfeng Reagent Company (China), $CdCl_2{\cdot}2.5H_2O$ was obtained from Shanghai Jinshanting New Chemical Reagent Company (China), and $NaBH_4$ and Te powder were acquired from Guoyao Chemical Reagent Company (China). The Pb^{2+} solution was prepared by dissolving 1.6594 g of $Pb(NO_3)_2$ in 50 mL doubly deionized water. Dilutions were made with doubly deionized water whenever necessary. A phosphate buffer solution (Na_2HPO_4-KH_2PO_4 0.067 mol L^{-1}, pH 7.4) was used in the experiments.

The synthesis of multicolor CdTe QDs

CdTe QDs were synthesized following a previous method [17]. Briefly, 50.0 mg $NaBH_4$, 3 mL anhydrous ethanol, 47.85 mg Te, and 1 mL doubly deionized water powder reacted in a small flask at 40 °C. Sodium hydrogen telluride (NaHTe) was produced. CdTe precursors were prepared by adding freshly prepared NaHTe solution to a N_2-saturated $CdCl_2$ solution at pH 8.0 in the presence of TGA as a stabilizing agent. The molar ratio of Cd^{2+}:Te^{2-}:TGA was 1:0.5:2.4. Further nucleation and growth of the QDs proceeded with refluxing at 100 °C under open air conditions with an attached condenser. Five fractions (QDs-I, QDs-II, QDs-III, QDs-IV, and QDs-V) were extracted at different times (10 min, 1 h, 4 h, 8 h, and 20 h, respectively) during reflux.

Procedures for fluorescence detection of Pb^{2+}

A phosphate buffer solution (pH=7.4) of about 800 μL and approximately 80 μL CdTe QDs-I were mixed thoroughly in a 10-mL volumetric flask. Two milliliters of the above solution were placed in a quartz cuvette, followed by a series of varying concentrations of Pb^{2+}. Fluorescence spectra were measured after the sample had reacted for 5 min at room temperature to obtain stable fluorescence intensities. Fluorescence spectra were obtained by an RF-5301 spectrofluorometer at an excitation wavelength of 325 nm. The slit width of excitation was 3 nm and the emission slit was 3 nm. Spectra of the other QDs (II–V) were also obtained based on similar procedure for the detection of Pb^{2+}.

Interference fluorescence quenching measurements

Doubly deionized water was used to prepare individual solutions of 0.5 μmol L^{-1} Ca^{2+}, Na^{+}, Mg^{2+}, K^{+}, Al^{3+}, Ba^{2+}, Zn^{2+}, and Fe^{3+}, and 0.1 μmol L^{-1} Hg^{2+}, Ag^{+}, and Cu^{2+}. Dual ionic interference studies were conducted by preparing a 10^{-7} mol L^{-1} solution mixture of Pb^{2+} and Ca^{2+}, Na^{+}, Mg^{2+}, Cu^{2+}, Al^{3+}, Ba^{2+}, Zn^{2+}, Hg^{2+}, Ag^{+}, Fe^{3+}, and K^{+}. Pb^{2+} was first introduced to the QDs, and then mixed with the various concentrations of ions. Characteristic spectra were obtained by the spectrofluorometer.

Detection of Pb^{2+} in spinach and citrus leaves

Spinach and citrus leaves were decomposed by dry digestion in a muffle furnace [22]. Solid samples were powdered and passed through 100 mesh sieves. These were then incinerated in porcelain crucibles until no smoke further emerged and calcined at 520 °C for 7–8 h in a muffle furnace. The ashes were dissolved using a 0.5 mol L^{-1} HNO_3 solution. The pH was adjusted to 7.4 with 0.1 mol L^{-1} NaOH solution, and 50 μL of the resulting solution was added to a CdTe QDs-I solution. The Pb^{2+} concentration of the final solution was then determined using the Stern-Volmer equation.

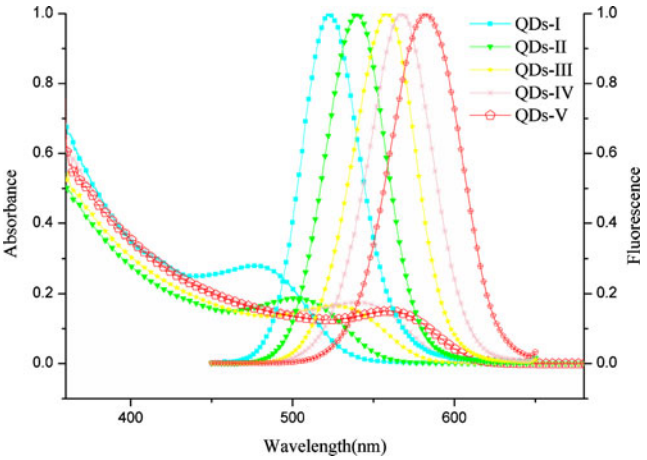

Fig. 1 Normalized emission fluorescence and absorption spectra of five different-sized CdTe QDs (QDs-I–V), λ_{ex}=325 nm

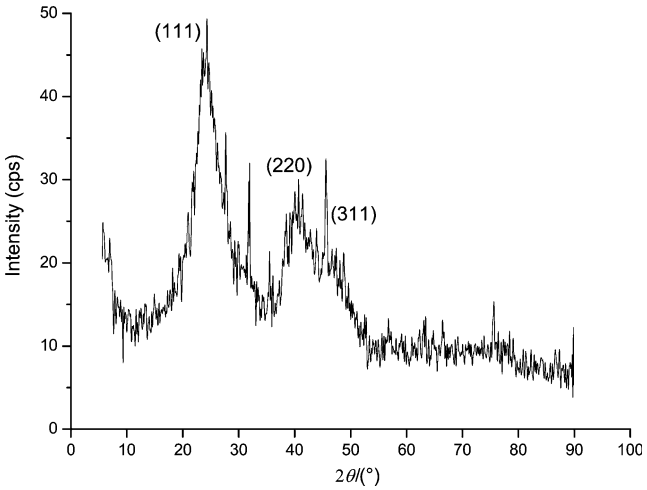

Fig. 3 XRD pattern of CdTe QDs-II

Results and discussion

Characterization of multicolor CdTe QDs

Figure 1 shows the fluorescence and absorption spectra of the QDs. The fluorescence emission peak appeared to red-shift from 520 to 595 nm after refluxing from 10 min to 20 h, indicating that the sizes of the CdTe QDs gradually increased. This was mainly due to the Ostwald ripening process, in which smaller particles dissolve and larger particles grow. The UV absorption spectra showed obvious first excitonic absorption peaks. This was due to the quantum confinement effect. The shapes of the emission wavelengths were symmetrical and smooth. The full width at half-maximum was less than 50 nm, indicating that the CdTe QDs had homogeneous sizes.

The morphology of CdTe QDs was studied by TEM. Figure 2a shows the surface characteristics of QDs-II, which was obtained by refluxing the CdTe QD solution for 1 h. The shapes of the nanoparticles were close to spherical and monodispersed. Their average particle diameter was about 2.5 nm, which coincided with the diameter calculated by the empirical formula in Ref. [23].

$$D = \left(9.8127 \times 10^{-7}\right)\lambda^3 - \left(1.7147 \times 10^{-3}\right)\lambda^2 + 1.0064\lambda - 194.84$$

where D (nm) is the diameter of the CdTe QDs, and λ (nm) is the wavelength of the first excitonic absorption peak. Using the formula above, the mean diameters of QDs-I, QDs-II, QDs-III, QDs-IV, and QDs-V were found to be 1.6, 2.4, 2.9, 3.1, and 3.3 nm, respectively. A typical electron diffraction ring image for QDs-II is shown in Fig. 2b. This image shows that the CdTe QDs possessed a good crystalline structure.

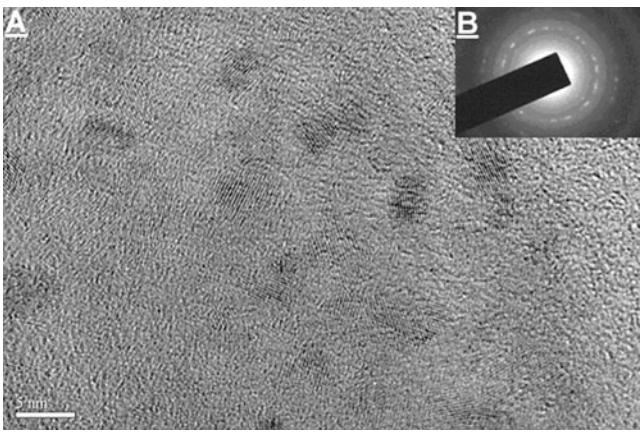

Fig. 2 **a** TEM image of CdTe QDs-II. **b** Electron diffraction ring of CdTe QDs-II

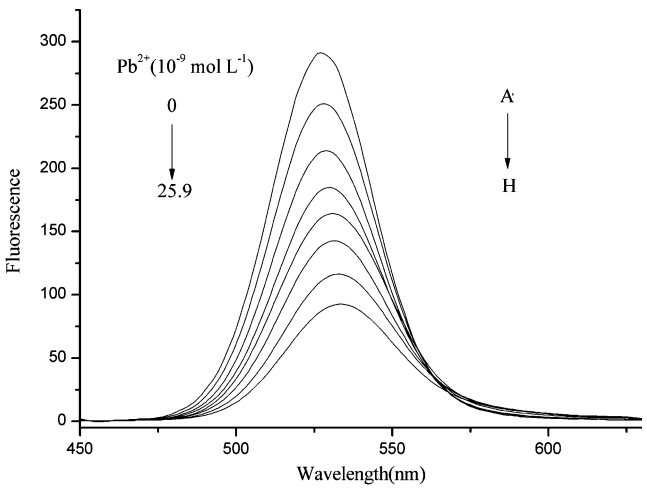

Fig. 4 Effect of Pb^{2+} concentrations on the luminescence of CdTe QDs-I: **A** 0, **B** 9.9×10^{-10} mol L^{-1}, **C** 1.96×10^{-9} mol L^{-1}, **D** 3.38×10^{-9} mol L^{-1}, **E** 5.66×10^{-9} mol L^{-1}, **F** 7.41×10^{-9} mol L^{-1}, **G** 1.30×10^{-8} mol L^{-1}, and **H** 2.59×10^{-8} mol L^{-1}

Table 1 Analytical parameters for the detection of Pb^{2+} using CdTe QDs-I–V

Probes	Sizes (nm)	FWHM (nm)	Regression equation	QY%	R^2	Linearange (nmol L^{-1})	LOD (nmol L^{-1})
I	1.6	38	$F_0/F = 9.74 \times 10^7 [Pb^{2+}] + 1.221$	30	0.9960	1.96–25.9	4.7
II	2.4	40	$F_0/F = 2.49 \times 10^6 [Pb^{2+}] + 1.011$	60	0.9924	1.96–333	268
III	2.9	43	$F_0/F = 2.92 \times 10^6 [Pb^{2+}] + 0.981$	51	0.9963	4.98–333	247
IV	3.1	47	$F_0/F = 2.39 \times 10^6 [Pb^{2+}] + 1.058$	44	0.9932	4.98–333	295
V	3.3	50	$F_0/F = 2.20 \times 10^6 [Pb^{2+}] + 1.026$	32	0.9921	4.98–285	218

Figure 3 shows the powder XRD pattern for CdTe QDs-II. The diffraction pattern of CdTe QDs was found to be relatively close to that of bulk cubic CdTe. The three diffraction peaks of the CdTe QDs at 23.6°, 40.2°, and 46.8° were respectively indexed to the (111), (220), and (311) planes of the cubic CdTe lattice.

The quantum yields of CdTe QDs were measured according to a previous method [24]. Rhodamin 6G, which was dissolved in anhydrous alcohol, was chosen as the standard sample. Experimental results showed that the quantum yields of CdTe QDs-I, -II, -III, -IV, and -V were 30%, 60%, 51%, 44%, and 32%, respectively.

The detection sensitivities of five colors of CdTe QDs towards Pb^{2+}

Figure 4 shows the fluorescence spectra of QDs-I with increasing Pb^{2+} concentrations. The fluorescence of QDs-I was gradually quenched with increasing Pb^{2+} concentration. While the fluorescence emission peak of QDs-I shifted by 6 nm to a longer wavelength, the fluorescence emission peaks of QDs-II–V did not apparently red-shift with the continuous addition of Pb^{2+}.

The surface of the QDs played an important role in their fundamental properties. For smaller particles, the surface atoms are chemically more active because they have fewer adjacent coordinate atoms and unsaturated sites or more dangling bonds. Therefore, the imperfection of the particle surface induces additional electronic states in the band gap, which act as electron or hole trap centers [17]. The obvious red-shift in the luminescence band of QDs-I in response to Pb^{2+} is attributed to effective electron transfers from thioglycolic acid to Pb^{2+} and the formation of a new radiative center [25].

The change in absorbance peak with increasing concentrations of Pb^{2+} solution is shown in Electronic Supplementary Material Fig. S1. The shape of QDs-I became asymmetrical after the addition of Pb^{2+} solution, which can be explained by static quenching [21].

QDs-I had a detection limit of 4.7 nmol L^{-1}, a sensitivity about 60 times greater than that of QDs-IV. QDs-II–V had proximate sensitivities, linear ranges, and detection limits for detecting Pb^{2+}. The related data are shown in Table 1.

The quenching efficiencies of five colors of CdTe QDs towards Pb^{2+}

Pb^{2+} quenched the fluorescence intensity of CdTe QDs in a concentration-dependent manner. This could be best described by the Stern-Volmer equation:

$$F_0/F = K_{SV}[Q] + 1,$$

where F_0 and F are the fluorescence intensity of CdTe QDs in the absence and presence of Pb^{2+}, respectively, K_{SV} is the

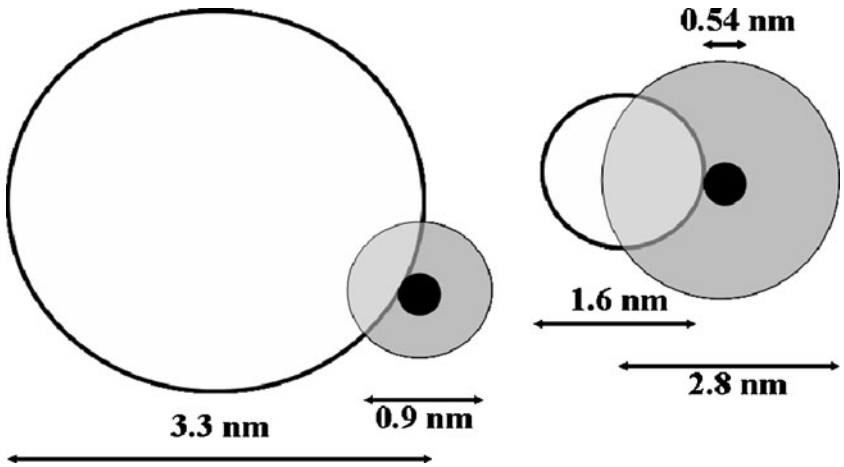

Fig. 5 Schematic representation of a molecule (black circle) positioned on the surface of red (3.3 nm) and green (1.6 nm) quantum dots. The grey circle represents the Perrin radii, interpreted as a sphere of action for the quencher

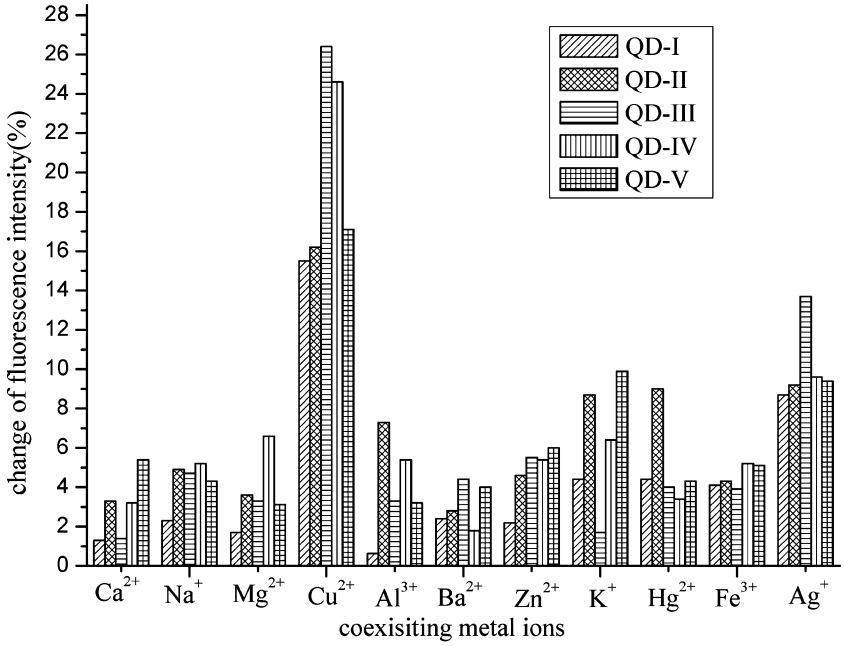

Fig. 6 Effect of metal ions on the fluorescence intensity of QDs-I–V in a phosphate buffer solution (pH=7.4) (the concentrations of Cu^{2+}, Hg^{2+} and Ag^{+} were 0.1 μmol L^{-1}, other ion concentrations were 0.5 μmol L^{-1})

Stern-Volmer quenching constant, which is related to the quenching efficiency, and [Q] is the concentration of Pb^{2+}.

A good linear relationship between F_0/F and [Q] can be seen from Electronic Supplementary Material Fig. S2. The K_{SV} of QDs-I was almost 40 times as large as those of QDs-II–V, and its quenching efficiency was the highest among the five colors. These findings were consistent with the report of Xia [26].

In CdTe QDs, the band gap, particle size, and surface curvature are related and can influence quenching process-

Table 2 Comparison of AAS and QDs-I methods for the detection of Pb^{2+} in spinach and citrus leaves

Agricultural products	QDs-I			AAS (mg/kg)	Content of coexisted ions (mg/kg)
	Content (mg/kg)	Average content (mg/kg)	RSD(%) (n=5)		
Spinach		14.43	4.8	12.01	Ca^{2+}(660±30)
					Na^{+}(1300±60)
	15.02				Mg^{2+}(552±15)
	13.51				Cu^{2+}(8.9±0.4)
	13.97				Al^{3+}(61±6)
	15.18				Ba^{2+}(9.0±0.8)
	14.46				Zn^{2+}(35.3±1.5)
					K^{+}(2490±110)
					Fe (540±20)
					Hg^{2+}(0.02±0.003)
Citrus leaves		11.44	4.2	10.62	Ca^{2+}(4200±400)
					Na^{+}(13±2)
					Mg^{2+}(234±7)
	11.63				Cu^{2+}(6.6±0.5)
	10.95				Al^{3+}(115±10)
	11.98				Ba^{2+}(98±6)
	11.71				Zn^{2+}(18±2)
	10.91				K^{+}(770±40)
					Fe (480±30)
					Ag^{+}(0.054±0.005)
					Hg^{2+}(0.150±0.02)

es. When the particle size reaches a certain measurement, the dimension may become a major factor affecting quenching efficiency [17]. In this case, the quenching radius is better viewed as the action radius for the quencher as it approaches the surface of the QDs. For smaller QDs (1.6 nm), a quencher can reach across most of the nanoparticles, whereas for larger QDs (3.3 nm), the quencher, given its quenching radius of only 0.45 nm, can only interact with excitons near a limited region of the surface. This is illustrated in Fig. 5. The large QD size-dependence of the quenching radius was a surprising discovery. We believe that such quenching could be partially controlled by the surface characteristics of the QD, notably its curvature [27]. QDs-I had the smallest-sized particles; thus, its quenching efficiency, which was 9.74×10^{7} mol^{-1} L, was the highest (Table 1).

The selectivities of five colors of CdTe QDs towards Pb^{2+}

Figure 6 shows that the fluorescence intensity of CdTe QDs was insensitive to Ba^{2+}, Hg^{2+}, Ag^{+}, and other physiologically important cations even if their concentrations were 500 times higher than that of Pb^{2+}. Only Pb^{2+} could effectively quench the fluorescence of CdTe QDs. The distinct discrimination between Pb^{2+} and other ions makes it possible for CdTe QDs to be used for the analysis of Pb^{2+} in the presence of other ions [28]. The results showed that QDs-I had a higher selectivity towards Pb^{2+} and that the influences of other metal ions, except Cu^{2+}, were much weaker. The presence of Cu^{2+} significantly influenced Pb^{2+} determination likely because of Cu^{+} formation, during which non-radiative recombination became easier among excited electrons in the conduction band and holes in the valence band, resulting in more powerful QD fluorescence quenching [29]. The selectivity of larger QDs was relatively low. Thus, QDs-I, which has the smallest size, is the most suitable for use as a probe for the detection of Pb^{2+}.

Detection of Pb^{2+} in spinach and citrus leaves

QDs-I was chosen to detect Pb^{2+} in spinach and citrus leaves. The results are shown in Table 2. The contents of Pb^{2+} in spinach and citrus were found to be 14.43 and 11.44 mg/kg, respectively. The QDs-I method showed an accuracy comparable with that of AAS, as no significant difference was found between the two methods when p=95% (t=0.103<$t_{0.05,4}$=2.776). In addition, coexisting ions, such as Ca^{2+}, Na^{+}, Mg^{2+}, Cu^{2+}, Al^{3+}, Ba^{2+}, Zn^{2+}, K^{+}, Hg^{2+}, Fe^{3+}, and Ag^{+}, yielded no interference within the allowable error range. Pb^{2+} recovery by QDs-I ranged from 92.2% to 107%, as shown in Table 3. Therefore, the QDs-method was accurate, sensitive, and selective for determining Pb^{2+}.

Conclusions

Multicolor water-soluble CdTe QDs modified by thioglycolic acid were synthesized. These CdTe QDs showed good distribution and displayed high fluorescence quantum yields. The experiment showed that the size of QDs influenced the detection sensitivity of Pb^{2+}. With increasing size of QDs, the sensitivity decreased. QDs-I, which was the smallest particle, had the highest quenching efficiency, selectivity, and sensitivity in the detection of Pb^{2+}; its detection limit was 4.7 nmol L^{-1}, which is the lowest in the current study. The larger QDs had wider linear ranges of 1.96×10^{-9}–3.33×10^{-7} mol L^{-1}. A new method using QDs-I for detecting Pb^{2+} in spinach and citrus leaves was established. Pb^{2+} amounts of 14.43 and 11.44 mg/kg were found in spinach and citrus, respectively. The results are in good agreement with those obtained with AAS. In summary, TGA-capped water-soluble CdTe QDs are excellent fluorescent probes for the detection of Pb^{2+}.

Table 3 Pb^{2+} concentrations in agricultural products as determined by AAS and QDs-I

Agricultural products	Amount of added standard sample Pb^{2+} (pmol)	Samples measured value (pmol)	The amount of actual measured (pmol)	Recovery (%)	RSD (%)
Spinach	2.00	1.32	3.21	94.95	2.2
	2.00	1.19	3.09	95.07	
	2.00	1.23	3.09	93.21	
	2.00	1.33	3.29	97.72	
	2.00	1.27	3.11	92.20	
Citrus leaves	2.00	2.04	4.17	106.7	3.5
	2.00	2.06	4.12	103.1	
	2.00	1.92	3.95	101.6	
	2.00	2.10	4.04	96.87	
	2.00	1.91	3.99	103.7	

Acknowledgement This work was financially supported by the National Natural Science Foundation of China (No. 20975050) and Jiangsu Province Program of Top-level Talents.

References

1. Maria AGT, Elvira MGL (2008) Toxic effects of perinatal lead exposure on the brain of rats: Involvement of oxidative stress and the beneficial role of antioxidants. Food Chem Toxicol 46 (6):2089–2095
2. Maren L, Jantje F, Franziska L, Corinna T, Martin S (2009) Chronic toxic demyelination in the central nervous system leads to axonal damage despite remyelination. Neurosci Lett 453(2):120–125
3. Pan YH, Liu XS, He XQ, Wang CH (2005) Lead speciation analysis by high performance liquid chromatography-inductively coupled plasma mass spectrometry. Chin J Anal Chem 33 (11):1560–1564
4. Zacharia A, Gucer S, Izgi B, Chebotarev A, Karaaslan H (2007) Direct atomic absorption spectrometry determination of tin, lead, cadmium and zinc in high-purity graphite with flame furnace atomizer. Talanta 72(2):825–830
5. Hsieh HF, Chang WS, Hsieh YK, Wang CF (2009) Lead determination in whole blood by laser ablation coupled with inductively coupled plasma mass spectrometry. Talanta 79:183–188
6. Pharmacopoeia C (2005 edition)
7. Baranowska I, Barchanska H, Pacak E (2006) Procedures of trophic chain samples preparation for determination of triazines by HPLC and metals by ICP-AES methods. Environ Pollut 143(2):206–211
8. Tian JN, Liu RJ, Zhao YC, Xu Q, Zhao SL (2009) Controllable synthesis and cell-imaging studies on CdTe quantum dots together capped by glutathione and thioglycolic acid. J Colloid Interface Sci 336:504–509
9. Jr MB, Moronne M, Gin P, Weiss S, Alivisatos AP (1998) Semiconductor nanocrystals as fluorescent biological labels. Science 281:2013–2016
10. Chan WCW, Nie SM (1998) Quantum dot bioconjugates for ultrasensitive nonisotopic detection. Science 281:2016–2018
11. Han MY, Gao XH, Su JZ, Nie SM (2001) Quantum-dot-tagged microbeads for multiplexed optical coding of biomolecules. Nature 19:631–635
12. Li Z, Dong CQ, Tang LC, Zhu X, Chen HJ, Ren JC (2010) Aqueous synthesis of CdTe/CdS/ZnS quantum dots and their optical and chemical properties. Luminesc. doi:10.1002/bio.1250
13. Yan ZY, Pang DW, Shao XF, Hu YZ (2005) Determination of trace amount of copper in the chinese herbal medicine by fluorescence quenching of quantum dots. J Chin Pharm Univ 36 (3):230–233
14. Gattás-Asfura KM, Leblanc RM (2003) Peptide-coated cds quantum dots for the optical detection of copper(II) and silver(I). Chem Comm 2684–2685
15. Zhang YY, Dong J, Wang N, Gao P, Zang SL (2009) The synthesis of luminescent CdTe quantum dots and its interaction with Au(III). Anal Sci 25(2):135–138
16. Pendyala NB, Koteswara Rao KSR (2009) Efficient hg and ag ion detection with luminescent PbS quantum dots grown in poly vinyl alcohol and capped with mercaptoethanol. Colloid Surf A 339:43–47
17. Zhong WY, Liang JR, Yu JS (2009) Systematic study of the interaction of cobalt ions with different-sized CdTe quantum dots. Spectrochim Acta Part A 74(3):603–606
18. Wang C, Zhao JW, Wang Y, Lou N, Ma Q, Su XG (2009) Sensitive Hg (II) ion detection by fluorescent multilayer films fabricated with quantum dots. Sensors Actuator B Chem 139 (2):476–482
19. Wu P, Li Y, Yan X (2009) Cdte quantum dots (QDs) based kinetic discrimination of Fe^{2+} and Fe^{3+}, and CdTe QDs-fenton hybrid system for sensitive photoluminescent detection of Fe^{2+}. Anal Chem 81(15):6252–6257
20. Mayra GV, Arístides CVG, Josefa AGC, Marta ED (2009) Analytical nanotechnology for food analysis. Microchim Acta 166:1–19
21. Wu HM, Liang JG, Han H (2008) A novel method for the determination of Pb^{2+} based on the quenching of the fluorescence of CdTe quantum dots. Microchim Acta 161:81–86
22. GB/T 5009.12-1996
23. Yu WW, Qu L, Guo W, Peng X (2003) Experimental determination of the extinction coefficient of CdTe, CdSe, and CdS nanocrystals. Chem Mater 15(14):2854–2860
24. Demas JN, Crosby GA (1971) The measurement of photoluminescence quantum yields. J Phys Chem 75(8):991
25. Burda C, Chen X, Narayanan R, El-Sayed MA (2005) The chemistry and properties of nanocrystals of different shapes. Chem Rev 105(4):1025–1102
26. Xia YS, Cao C, Zhu CQ (2008) Two distinct photoluminescence responses of CdTe quantum dots to Ag (I). J Luminesc 128 (1):166–172
27. Scaiano JC, Laferriere M, Galian RE, Maurel V, Billone P (2006) Non-linear effects in the quenching of fluorescent semiconductor nanoparticles by paramagnetic species. Phys Stat Sol (A) 203 (6):1337–1343
28. Lai SJ, Chang XJ, Fu C (2009) Cadmium sulfide quantum dots modified by chitosan as fluorescence probe for copper (II) ion determination. Microchim Acta 165:39–44
29. Isarov A, Chrysochoos J (1997) Optical and photochemical properties of nonstoichiometric cadmium sulfide nanoparticles: surface modification with copper(II) ions, vol 13. American Chemical Society, Washington, DC, ETATS-UNIS